Climate Dynamics (2005) 25: 401–413
DOI 10.1007/s00382-005-0049-9

M. Vuille · M. Werner

Stable isotopes in precipitation recording South American summer monsoon and ENSO variability: observations and model results

Received: 25 January 2005 / Accepted: 16 May 2005 / Published online: 9 July 2005

Abstract The South American Summer Monsoon (SASM) is a prominent feature of summertime climate over South America and has been identified in a number of paleoclimatic records from across the continent, including records based on stable isotopes. The relationship between the stable isotopic composition of precipitation and interannual variations in monsoon strength, however, has received little attention so far. Here we investigate how variations in the intensity of the SASM influence $\delta^{18}O$ in precipitation based on both observational data and Atmospheric General Circulation Model (AGCM) simulations. An index of vertical wind shear over the SASM entrance (low level) and exit (upper level) region over the western equatorial Atlantic is used to define interannual variations in summer monsoon strength. This index is closely correlated with variations in deep convection over tropical and subtropical South America during the mature stage of the SASM. Observational data from the International Atomic Energy Agency-Global Network of Isotopes in Precipitation (IAEA-GNIP) and from tropical ice cores show a significant negative association between $\delta^{18}O$ and SASM strength over the Amazon basin, SE South America and the central Andes. The more depleted stable isotopic values during intense monsoon seasons are consistent with the so-called ''amount effect'', often observed in tropical regions. In many locations, however, our results indicate that the moisture transport history and the degree of rainout upstream may be more important factors explaining interannual variations in $\delta^{18}O$. In many locations the stable isotopic composition is closely related to El Niño-Southern Oscillation (ENSO), even though the moisture source is located over the tropical Atlantic and precipitation is the result of the southward expansion and intensification of the SASM during austral summer. ENSO induces significant atmospheric circulation anomalies over tropical South America, which affect both SASM precipitation and $\delta^{18}O$ variability. Therefore many regions show a weakened relationship between SASM and $\delta^{18}O$, once the SASM signal is decomposed into its ENSO-, and non-ENSO-related variance.

M. Vuille (✉)
Climate System Research Center, Department of Geosciences, Morrill Science Center, University of Massachusetts, 611 North Pleasant Street, Amherst, MA, 01003-9297 USA
E-mail: mathias@geo.umass.edu
Tel.: +1-413-5450659
Fax: +1-413-5451200

M. Werner
Max Planck Institute for Biogeochemistry, Jena, Germany

1 Introduction

The South American Summer Monsoon (SASM) is a major component of the climate system over tropical and subtropical South America during austral summer. Although not as famous as its counterpart over Asia, the SASM has recently gained recognition as a dominant regional circulation feature which contains many of the typical monsoon characteristics (Zhou and Lau 1998). These features, which are best developed during the summer months December–February (DJF), include a large-scale land-ocean temperature gradient, low pressure over the interior of the continent (Chaco low) and high pressure (Bolivian High) with anticyclonic circulation aloft, a vertically overturning circulation with a rising branch over the interior of the continent and sinking motion over the ocean, and intense moisture influx to the continent at low levels responsible for strong seasonal precipitation changes. Over much of tropical and subtropical South America more than 50% of the annual precipitation falls during the summer months, associated with the establishment of the SASM. As a monsoon system the SASM is dynamically and geographically different from the maritime ITCZ, although the latter is sometimes erroneously invoked to

explain the seasonal march of precipitation over the South American continent.

On interannual and longer timescales summer precipitation shows significant variations in intensity and spatial extent, which are still not very well understood. This variability is caused by a number of factors influencing the SASM during both the developing and mature stage, including tropical Atlantic sea surface temperatures (SST) (e.g. Mechoso et al. 1990; Hastenrath and Greischar 1993; Marengo and Hastenrath 1993; Vuille et al. 2000a), the El Niño-Southern Oscillation (ENSO) (e.g. Aceituno 1988; Vuille 1999; Garreaud and Aceituno 2001; Paegle and Mo 2002; Grimm 2003, 2004; Lau and Zhou 2003), land surface conditions such as soil moisture or vegetation cover (e.g. Oyama and Nobre 2003; Koster et al. 2004) and interactions with the extratropical circulation (e.g. Garreaud and Wallace 1998; Seluchi and Marengo 2000; Chou and Neelin 2001). The relative importance of the various factors contributing to SASM variability, however, is often difficult to determine, as many components such as tropical Pacific and Atlantic SST are intrinsically linked with each other (e.g. Enfield 1996; Uvo et al. 1998; Vuille et al. 2000b; Pezzi and Cavalcanti 2001; Giannini et al. 2001; Ronchail et al. 2002). The growing interest in the SASM has also been fueled by a number of recent paleoclimatic records emerging from the central Andes, a region ideally located to study SASM variability as it receives 70–80% of its annual precipitation during the summer months (Vuille et al. 2000b; Garreaud et al. 2003). These proxy data provide evidence for dramatic regional-scale changes in austral summer precipitation on centennial to millennial time scales (e.g. Betancourt et al. 2000; Baker et al. 2001; Fritz et al. 2004; Rowe and Dunbar 2004). Stable water isotope records (δ^{18}O and δD) from lake sediments (e.g. Abbott et al. 2000; Seltzer et al. 2000), fluid inclusions (e.g. Godfrey et al. 2003); ice cores (e.g. Thompson et al. 1985, 1995, 1998; Ramirez et al. 2003) or speleothems (e.g. Cruz et al. 2005a) are amongst the most prominent indicators of such past variations of the SASM. The interpretations of these records, however, are not always consistent with each other, largely because the correct interpretation of stable water isotopes in the tropics is still a matter of debate (e.g. Hoffmann 2003).

Atmospheric General Circulation Models (AGCMs) fitted with stable isotopic tracers, in combination with observational data, have helped to significantly advance our understanding of what controls δ^{18}O and δD variability in tropical precipitation over South America (e.g. Vuille et al. 2003a). So far, ice cores from the tropical Andes have been at the center of this debate. Bradley et al. (2003), Hoffmann et al. (2003) and Vuille et al. (2003b) have all emphasized the significant influence of ENSO and tropical Pacific SSTs upon ice core δ^{18}O, through its impact on the atmospheric circulation aloft the central Andes and on the stable isotopic content of mid-tropospheric water vapor upstream over the Amazon basin.

The goal of this study is to reexamine the association between the SASM and the stable isotopic composition of δ^{18}O over the entire tropical South American continent, and to determine the relative influence of the remote forcing (ENSO) upon both SASM and δ^{18}O. We make use of the same high-resolution atmospheric AGCM (ECHAM-4 in T106 spectral resolution) that was successfully applied in Vuille et al. (2003a, b) over tropical South America. In addition we compare our model results with the available observational data from ice cores and the International Atomic Energy Agency-Global Network of Isotopes in Precipitation (IAEA-GNIP) data base (IAEA/WMO 2004). In the next section we present the data and methods that were used. Section 3 describes the main features of the SASM in more detail and shows how we define interannual variations in SASM strength. In Sect. 4 we discuss how the stable isotopic composition of austral summer precipitation over South America is related to the strength of the SASM, while Sect. 5 deals with the relative importance of ENSO upon SASM and δ^{18}O. Section 6 ends with a discussion and some concluding remarks.

2 Data and methods

The AGCM used in this study is the high-resolution version of the ECHAM-4 stable isotope model (Hoffmann et al. 1998). It is a spectral model, based on a hybrid sigma-pressure coordinate system and was run with triangular truncation at wave-number 106 (spatial resolution $\backsim$1.1°latitude × 1.1°longitude), including 19 vertical layers from surface to 30 hPa. The model was run under modern boundary conditions and forced with observed global SST data [global sea-ice and sea surface temperature (GISST) 2.2] between 1979 and 1998. The first year (1978) was discarded to avoid data problems with model equilibration during spin-up time. The same model has already been successfully applied over the tropical Americas in previous studies (Vuille et al. 2003a, b).

To validate the model simulations we extracted monthly means of δ^{18}O in precipitation from all stations in South America, which contained at least ten summers (DJF) worth of data in the IAEA-GNIP data base (IAEA/WMO 2004). This observational network was completed by adding annually resolved δ^{18}O values from the tropical Andean ice cores Quelccaya (13°56′S, 70°50′W), Huascarán (9°06′S, 77°30′W) and Sajama (18°06′, 68°53′W) (Thompson et al. 1985, 1995; Hardy et al. 2003). While these records are not exclusively recording summer (DJF) precipitation, the large majority of snowfall occurs during austral summer (Vuille et al. 2003b) and most of the occasional winter snowfall is not retained in these records as wind scour and sublimation are high. Wagnon et al. (2003) have documented that wintertime sublimation ranges between 0.7 mm day^{-1} and 1.2 mm day^{-1} in the eastern Bolivian Andes and Hardy et al. (2003) have shown that, at least

on Sajama, no snowfall is retained outside a narrow time window between November and February. Hence we view these ice core records as strongly biased toward the wet season and indicative of austral summer conditions.

To describe variations in the large-scale circulation associated with the SASM we used global reanalysis data (Kalnay et al. 1996) between 1950 and 2004 from the National Centers for Environmental Prediction-National Center for Atmospheric Research (NCEP-NCAR). This data set is available on a 2.5° × 2.5° horizontal grid with 17 vertical pressure levels.

Precipitation and convective activity associated with the SASM were analyzed based on monthly Climate Prediction Center (CPC) Merged Analysis of Precipitation (CMAP; Xie and Arkin 1997) and NOAA interpolated Outgoing Longwave Radiation (OLR) data (Liebmann and Smith 1996). CMAP data is available since 1979 on a 2.5° × 2.5° horizontal grid and represents a blend of observational in-situ raingauge measurements with satellite data. OLR data is equally available on a global 2.5°latitude × 2.5°longitude grid since 1974, with several months in 1978 missing. Measured at the top of the atmosphere by satellites, OLR is indicative of the energy emitted by the earth's surface and a commonly used proxy for convective activity in the tropics. We used CMAP and OLR data rather than NCEP-NCAR precipitation because they are based entirely (OLR) or at least partially (CMAP) on observations. NCEP-NCAR precipitation on the other hand is a model-based variable, which shows deficiencies in both its seasonal cycle as well as the spatial pattern near the Andes (Costa and Foley 1998; Liebmann et al. 1998). An index of tropical Pacific SSTA, Niño 3.4, representing the average SSTA over the domain (5°N–5°S, 120°–170°W) was used to document the relationship of the SASM and the stable isotopic composition of precipitation with ENSO.

3 The South American summer monsoon (SASM)

Consistent with the seasonal cycle of solar radiation a precipitation maximum develops over the southern Amazon region in late spring. While the demise of summer precipitation is characterized by an almost constant northward migration of the zone of maximum precipitation, the onset of precipitation south of the equator during late spring is rather abrupt (Fig. 1a). This sudden establishment of a summer precipitation regime over the southern tropics and subtropics of South America is associated with the onset of the SASM (Zhou and Lau 1998; Gan et al. 2004). Concurrent with the weakening and southward displacement of the subtropical jetstream due to the weakened meridional temperature gradient, the Bolivian High is established east of the central Andes as a Rossby wave response to the increased latent heat release over the Amazon basin (Silva Dias et al. 1983; Lenters and Cook 1997). At the height of the SASM season (DJF) strongest convective activity is centered over the central Andes and the southern Amazon basin (Fig. 2a). In the lower troposphere a heat low with cyclonic activity develops to the east of the central Andes. The trade winds emanating from the Sahara high are strengthened and transport increased moisture from the tropical North Atlantic toward the continent (Fig. 2b). Upon reaching the tropical Andes, these winds are deflected toward the southeast and provide an efficient conveyor belt for southward transport of moisture along the eastern slopes of the Andes. Outflow from the Bolivian High acts as an upper-air monsoonal return flow directed northward east of the Bolivian High and curving east toward North Africa around the Nordeste Low (Fig. 2a).

The ECHAM-4 model quite accurately simulates summertime climate over tropical South America (Vuille et al. 2003a). The major deficiency in the model is the underestimation of precipitation amounts at the height of the SASM season (Fig. 1b). Both the timing and the spatial extent of the SASM are, however, quite accurately reproduced. As we will show, interannual variability of precipitation and atmospheric circulation related to the SASM are also simulated reasonably well by the model. For further discussions of model performance over tropical South America we refer the reader to Vuille et al. (2003a).

To assess how interannual variability in monsoon strength and stable isotopic composition of precipitation

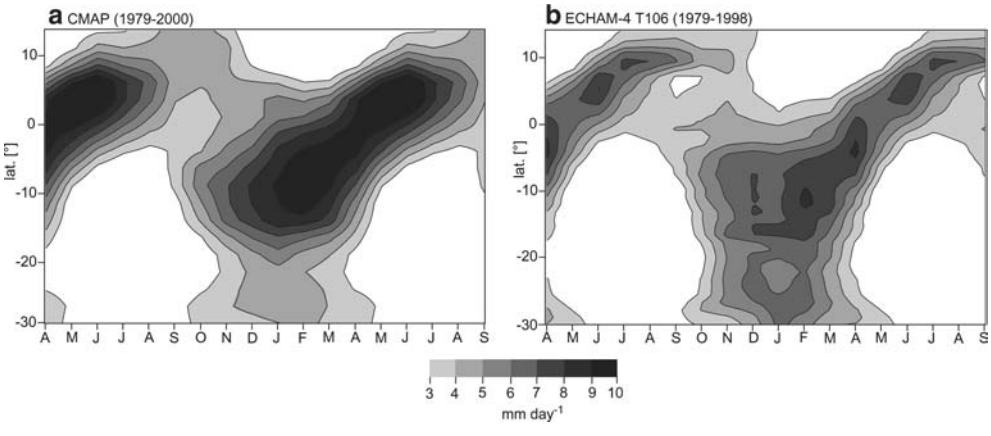

Fig. 1 Time-latitude diagram of the seasonal cycle of precipitation (in mm day^{-1}) averaged over longitude 50°–70°W for **a** CMAP (1979–2000) and **b** ECHAM-4 T106 (1979–1998). Contour interval is 1 mm day^{-1}; only precipitation > 3 mm day^{-1} is shown

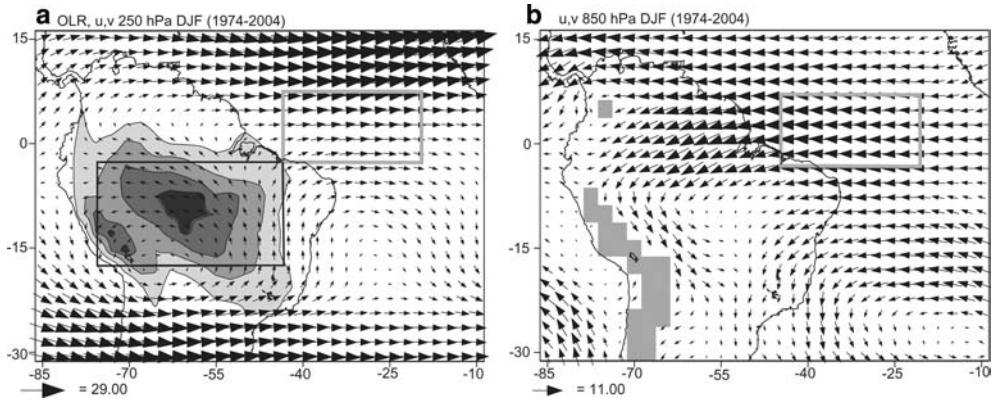

Fig. 2 **a** DJF OLR and 250 hPa wind (1974–2004). Contour intervals and gray shading indicate 225, 210, 200 and 195 W m^{-2}, respectively. Vector for wind field (in m s^{-1}) is shown in *lower left*. **b** the DJF 850 hPa wind (*gray shading* indicates regions >1,500 m in NCEP model topography). *Black box* in (**a**) shows region of convective index CI (2.5–17.5°S/45–75°W) and *gray box* shows regions of strongest vertical shear (7.5°N–2.5°S/45–20°W) in (**a**) and (**b**)

are related with each other, a quantitative measure of the SASM is needed. Here we define monsoon intensity as the strength of convective activity over the center of summer convection displayed in Fig. 2a. A convective index (CI) is defined as the negative DJF OLR departures (with respect to the annual cycle), averaged over the region 2.5°–17.5°S; 45°–75°W (black box in Fig. 2a). We use negative OLR anomalies to ensure that the CI will be positively correlated with monsoon strength (the more negative OLR values are, the more intense is deep convection).

Unfortunately this CI can only be extended back to 1974, the year when observations of OLR began, while much of the stable isotope data from the IAEA–GNIP stations in South America stem from the 1960s and early 1970s. Hence a meaningful comparison of monsoon strength based on the CI with the stable isotopic composition of precipitation is not possible. To circumvent this problem we tie the strength of convective activity over tropical South America to the large-scale atmospheric circulation, for which reanalysis data is available dating back to 1948. A similar approach was presented by Wang and Fan (1999) over Asia. They suggested considering the centers of deep monsoonal convection and then defined a vertical shear index over the region which is most closely related to this center of convection. Such an approach is dynamically consistent with viewing the vertical wind shear as a first-order baroclinic Rossby wave response to latent heat release in the mid-troposphere during monsoon precipitation (Gill 1980; Webster and Yang 1992). Here we follow the methodology of Wang and Fan (1999) by regressing the CI time series with the upper and lower tropospheric wind field and with the vertical shear between 850 hPa and 250 hPa zonal wind.

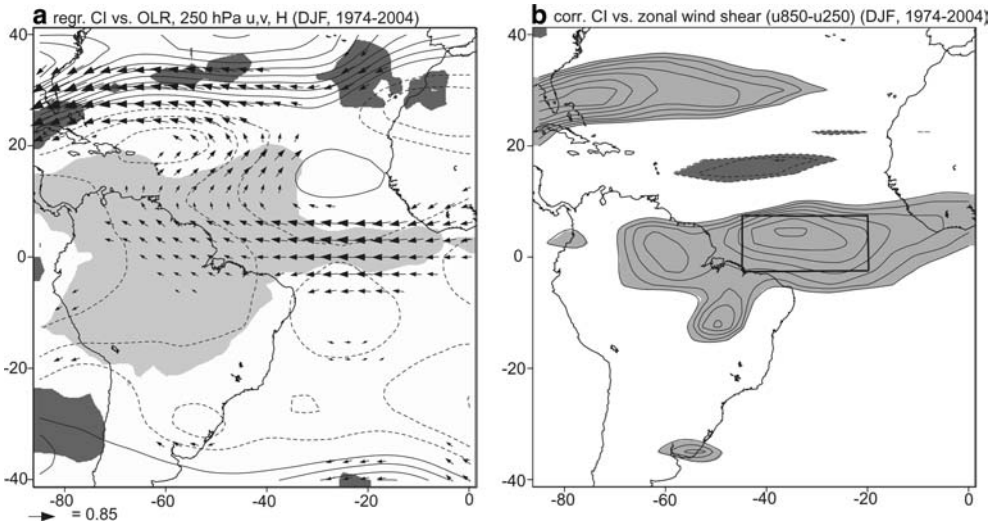

Fig. 3 Regression of CI with **a** DJF OLR, 250 hPa *u*, *v* and geopotential height (H), **b** correlation of CI with zonal shear (u_{850}–u_{250}). Scale for wind vectors (in m s^{-1} per SD) in (**a**) is shown in *lower left*. Wind vectors are only shown where correlation of either zonal or meridional component with CI is significant at $p = 0.05$. Contour interval for *H* is 0.5 gpm per SD; negative contours are *dashed*. *Shading* in (**a**) indicates significant positive (*dark gray*) or negative (*light gray*) correlation ($p = 0.05$) between CI and OLR. Shading in b) indicates significant positive (*light gray*) or negative (*dark gray*) correlation ($p = 0.05$) between CI and zonal shear. Contour interval in (**b**) is 0.04 and omitted where insignificant (between −0.36 and 0.36). *Black box* indicates region of zonal shear index (7.5°N–2.5°S/45–20°W)

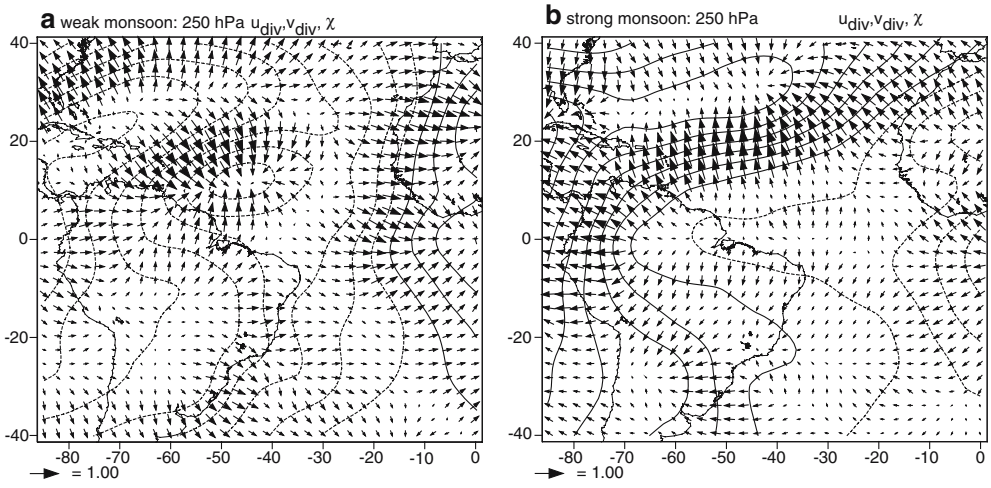

Fig. 4 **a** the DJF 250 hPa composite of divergent wind (u_{div},v_{div}) and velocity potential (χ) during five weakest monsoon summers between 1950 and 1998 (1976/1977, 1977/1978, 1980/1981, 1982/1983, 1986/1987) as defined by M_{obs}, (**b**) as in (**a**) but for five strongest monsoon summers (1961/1962, 1962/1963, 1973/1974, 1975/1976, 1988/1989). Contour interval for velocity potential is 2×10^6 m^2 s^{-1} per SD; negative contours are *dashed*. Scale for divergent wind vector is shown in *lower left* of each Figure

Figure 3 shows how variations in deep convection over tropical South America are related to the upper tropospheric circulation (Fig. 3a) and to the zonal wind shear (Fig. 3b). The OLR field in Fig. 3a shows that convective activity associated with a strong SASM is not only enhanced over the entire tropical continent, but is also linked to intensified convection over the Atlantic Intertropical Convergence Zone (ITCZ). The most conspicuous feature in the upper troposphere are the weakened subtropical westerly jet and anomalous tropical easterlies. In the lower troposphere (not shown) a strong SASM in DJF is related to a deepening of the subtropical low pressure cell and intensified cyclonic circulation over the southeast of the continent, a pattern that can also be traced back to individual wet events (Gan et al. 2004). Figure 3b shows the correlation between CI and the zonal wind shear (u_{850}–u_{250}). The strongest positive correlation is located over the entrance (low level) and exit (upper level) region of the SASM (see gray box in Fig. 2). This region coincides with the area of strongest upper-air divergent outflow and mid-tropospheric ascending motion during austral summer (Hastenrath 2001). Hence we define a monsoon-index M_{obs} based on the vertical wind shear derived from zonal wind anomalies at the 850 and 250 hPa level (u_{850}–u_{250}) averaged over the region 7.5°N–2.5°S/45–20°W (black box in Fig. 3b). The positive correlation pattern in Fig. 3b indicates that enhanced tropical convection during a strong monsoon summer is associated with anomalous upper level easterly and anomalous low-level westerly flow. This is consistent with results by Gan et al. (2004), who showed that the austral summer wet season over the southern Amazon basin is associated with the sudden establishment of upper-air easterlies and low-level westerly winds over the region. To better characterize the differences between weak and strong monsoon summers, Fig. 4 shows composites of the divergent upper-air circulation based on ensembles of the five strongest and weakest monsoons summers as defined by the timeseries of M_{obs} between 1950 and 1998. The most conspicuous features during weak monsoons are the strong upper-air convergence and related sinking motion located just off the coast of northern South America as shown in the composite of 250 hPa divergent wind and velocity potential (Fig. 4a). This large-scale upper-tropospheric convergence, in conjunction with the shallow equatorial trough (not shown) is consistent with the suppressed convective

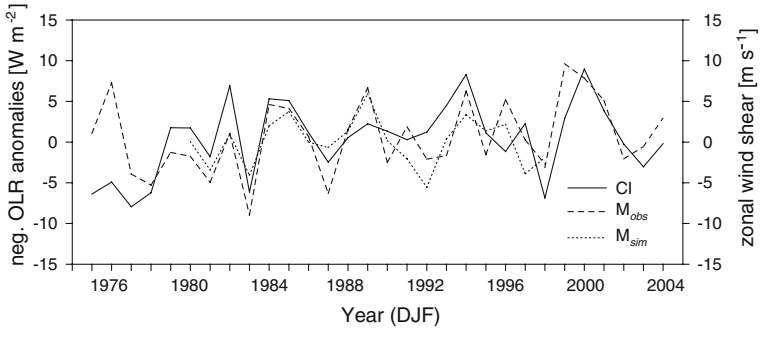

Fig. 5 Comparison of CI with reanalysis-derived Monsoon index M_{obs} and ECHAM-4 T106 derived Monsoon index M_{sim}(DJF, 1974–2003)

activity over the tropical Atlantic and tropical South America during weak monsoon years as seen in the OLR data (Fig. 3a). During strong monsoon years on the other hand, a zonal band of large-scale upper-air divergence, low-level convergence (not shown) and associated ascending motion is located over the equatorial Atlantic and extends westward over the tropical continent (Fig. 4b). Again this is consistent with the significantly enhanced convective activity seen in the OLR data (Fig. 3a). These monsoon-related anomalies seen in the divergent circulation are in agreement with the notion of a zonally overturning circulation, which develops in this sector of the tropical Atlantic during austral summer (Hastenrath 2001).

Overall the monsoon patterns described in Figs. 3 and 4 show that our vertical shear index M_{obs} captures the main large-scale circulation anomalies associated with the SASM. Since we will use M_{obs} as index for SASM strength in the remainder of this study, it is important to see how closely this index correlates with the previously established convective index. The correlation of M_{obs} with CI over the instrumental period 1974–2004 is 0.55, significant at $p = 0.01$ (Fig. 5). Despite this significant relationship, however, large discrepancies exist between CI and M_{obs} in certain years. It is noteworthy that the periods of largest departures between the zonal shear index and the convective index (1974/75, 1975/1976, 1988/1989, 1995/1996 and 1998/1999) all coincide with La Niña events (Trenberth 1997). In each case the zonal shear index indicated a strong SASM, which was not evident in the convective index. The significant influence that La Niña events seem to have on the relationship between CI and M_{obs} is reflected in the correlation between the two variables, which increases to 0.78 ($p = 0.001$), when these 5 years are omitted. The fact that our monsoon-index does not accurately capture

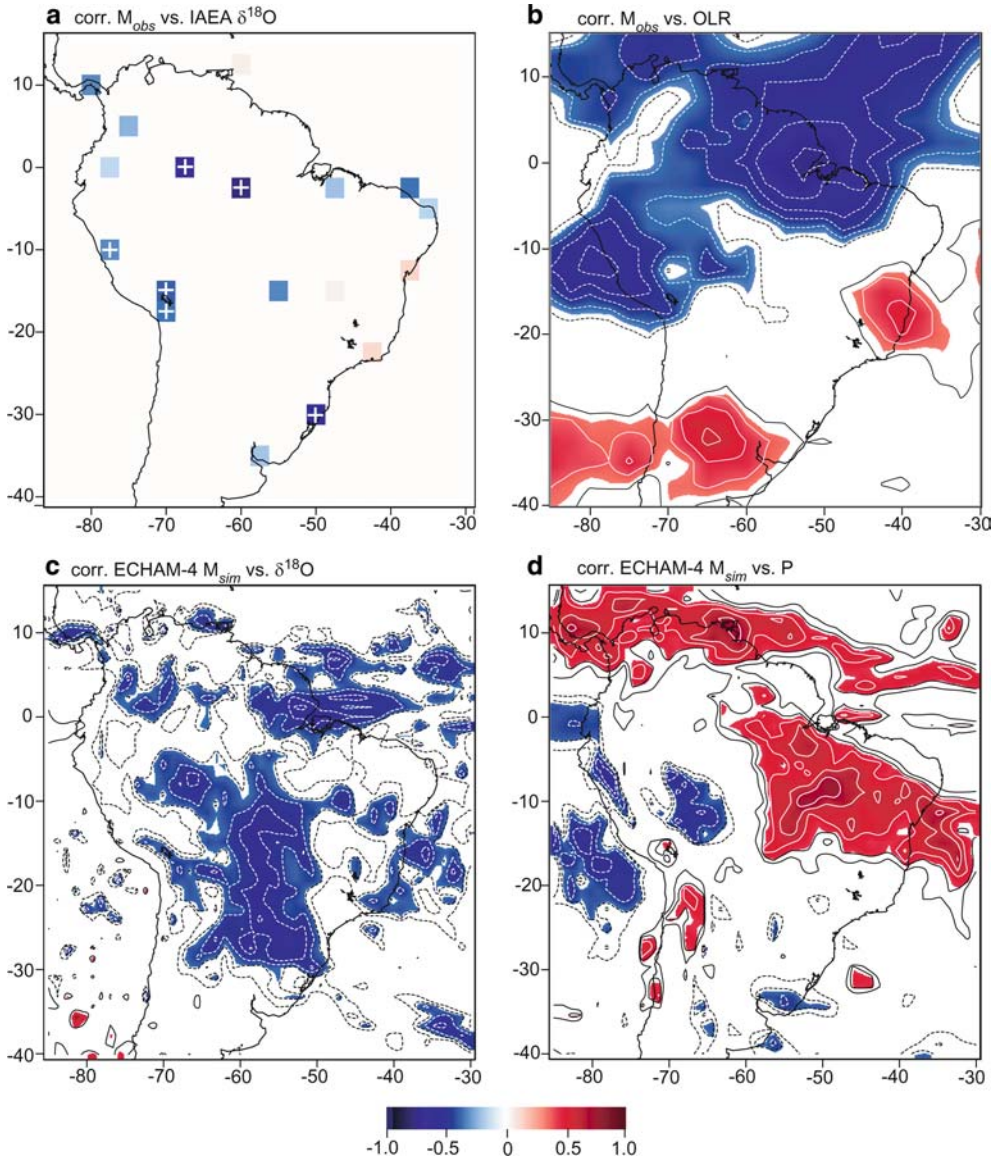

Fig. 6 **a** Correlation of M_{obs} with DJF IAEA $\delta^{18}O$ and ice core $\delta^{18}O$ from Huascarán, Quelccaya and Sajama (varying record lengths) **b** correlation of M_{obs} with DJF OLR (1974–2004), **c** correlation of $M_{sim}$with ECHAM-4 T106 $\delta^{18}O$ (1979–1998), **d** correlation of M_{sim} with ECHAM-4 T106 precipitation (1979–1998). Contour interval in (**b**), (**c**) and (**d**) is 0.1; contours between 0.2 and −0.2 are omitted; *negative contours* are *dashed*, and significant negative (*positive*) correlations ($p = 0.05$) are *shaded in blue* (*red*). Significant correlations in (**a**) are indicated with *white cross*

convective activity over tropical South America during La Niña events is a limitation of our study, which should be kept in mind when interpreting the results. We will discuss the ENSO influence on M_{obs} in more detail in Sects. 5 and 6.

Finally it is noteworthy to observe that the ECHAM-4 model is able to quite accurately portray monsoon variability as defined above. We derive a similar index M_{sim} in the model, which is highly correlated with M_{obs} over the 20 years of model integration ($r = 0.73$, $p = 0.001$, Fig. 5). This is in support of previous results by Vuille et al. (2003a), showing that the ECHAM-4 model is able to reasonably well simulate interannual climate variability over the tropical Americas. The correlation of $M_{sim}$with CI ($r = 0.52$, $p = 0.05$; Fig. 5) is similar to the observed correlation between M_{obs} and CI and again points to the bias introduced by La Niña conditions, as the correlation improves substantially ($r = 0.62$, $p = 0.01$) if the two La Niña periods 1988/89 and 1995/96 are omitted.

4 The SASM and $\delta^{18}O$

Given that the zonal wind shear index M_{obs} is a reasonably accurate descriptor of the summer monsoon strength over South America and that the ECHAM-4 model is able to correctly simulate its interannual variability as observed in the reanalysis data, we next investigate how SASM strength (as defined by M_{obs}) relates to the stable isotopic composition in both observational and model data. It is important, however, to keep in mind that the $\delta^{18}O$ data from the IAEA network represents varying record lengths (although at least 10 years long) over different time periods, while results based on the ECHAM-4 model are always based on the same 20 years, 1979–1998.

We first compare the relationship between $\delta^{18}O$ and SASM in both observations and model (Fig. 6). The IAEA-GNIP data indicates that the South American monsoon is negatively correlated with $\delta^{18}O$ over the entire continent, except along the east coast of Brazil between 10° and 20°S (Fig. 6a). Significant negative correlations (highlighted with a white cross) are evident over the Amazon basin (Manaus, 3.12°S, 60.02°W and Sao Gabriel, 0.13°S, 67.08°W), the central Andes (ice core data from Huascarán, Quelccaya and Sajama) and over southeastern South America (Porto Alegre, 30.08°S, 51.18°W). The model results are consistent with the results obtained from the sparse observational IAEA network. The model simulates a similar negative relationship between SASM (M_{sim}) and $\delta^{18}O$ over the entire continent, with highly significant correlations over parts of the Amazon basin, the Altiplano region and most of subtropical South America, including southeastern South America (Fig. 6c). The weak positive correlations along the east coast, however, are not evident in the model.

The fact that a strong summer monsoon leads to more negative $\delta^{18}O$ values is consistent with the so-called "amount effect" (Dansgaard 1964). As shown by Vuille et al. (2003a) most tropical and subtropical locations in South America do indeed exhibit a significant "amount effect" on interannual timescales with more depleted $\delta^{18}O$ values in wet years and more enriched $\delta^{18}O$ values during dry years. Correlation of M_{obs} and M_{sim} with OLR and simulated precipitation however, only partially supports this notion (Fig. 6b, d). A stronger monsoon is obviously related to enhanced convective activity over the South American tropics, as evidenced by the significant negative correlation between M_{obs} and OLR over the Amazon basin, the tropical North Atlantic and the central Andes (Fig. 6b). Hence the negative correlation between M_{obs} and $\delta^{18}O$ over these regions may indeed be related to the amount effect, when condensation and fractionation take place during the vertical ascent of air masses in small-scale convective cloud systems. $\delta^{18}O$ values over southeastern South America (Porto Alegre), however, are also significantly negatively correlated with the strength of the summer monsoon, even though there is no indication of increased precipitation in the OLR data, consistent with results by Cruz et al. (2005b). On the contrary there is a significant dipole pattern with enhanced convective activity in the tropics and subdued convection in the subtropics during a strong SASM and vice versa; a pattern detected in a number of previous studies and related to ENSO (e.g. Paegle and Mo 2002). Summer precipitation in Porto Alegre is related to an intensified southward transport of moisture from the tropics. Hence strong convective activity and associated rainout of heavy isotopes upstream over the Amazon basin will lead to a depletion of the remaining water vapor. As shown by Vuille et al. (2003a) such a rainout process and isotopic depletion along the trajectory of an air mass does indeed occur over South America, although it is weaker than in mid-latitudes due to the dominance of non-fractionating evapotranspiration over evaporation in the Amazon basin. This depleted moisture is subsequently transported southward along the eastern slopes of the Andes and will lead to more negative $\delta^{18}O$ values over southeastern South America, even if local precipitation amounts are not very high. This mechanism points toward the crucial role of moisture transport history and the degree of rainout upstream. It also shows that caution is needed when interpreting the stable isotopic composition of precipitation in the tropics and that the "amount effect" alone is insufficient to explain many aspects of monsoon-related $\delta^{18}O$ variability. Our model simulations support this notion as several locations (e.g. southeastern South America or the southwestern Amazon basin near the eastern Andean slope) show significantly depleted $\delta^{18}O$ values associated with a strong monsoon (Fig. 6c), even though precipitation over these regions is reduced (Fig. 6d). Clearly this effect becomes more important for distant regions, which are located farther away from the original

moisture source. Here the degree of rainout during transport is probably more important than the "amount effect" since strong rainout during active monsoon years over the eastern Amazon basin preconditions the stable isotopic composition of precipitation downstream.

5 The ENSO signal in the SASM

Both observations and model results seem to indicate a significant negative relationship between SASM strength and the stable isotopic composition of tropical Andean ice cores. On the other hand Vuille et al. (2003a), Hoffmann et al. (2003) and Bradley et al. (2003) have convincingly argued for a strong impact of ENSO on the $\delta^{18}O$ variability in these records. Hence it is worthwhile to take a closer look at how ENSO, SASM and $\delta^{18}O$ compare in some of the records where Fig. 6 suggested a significant relationship. Figure 7 shows the timeseries of available $\delta^{18}O$ data for Manaus, Porto Alegre (both averaged over DJF) and from the Sajama ice core. The data are compared with both monsoon strength (left column) and with ENSO (right column). As already shown in Fig. 6a all three observational records are significantly negatively correlated with M_{obs}. In the case of both Manaus and Sajama, however, the correlation with the ENSO index Niño 3.4 is as strong as with the SASM. Only the record from Porto Alegre is significantly affected by the SASM but not by ENSO. Furthermore, multiple stepwise linear regression analyses (not shown) indicate that the explained variance in the Manaus and Sajama $\delta^{18}O$ records does not significantly increase if both SASM and ENSO enter the model as predictors. Hence it appears as if these two variables by and large explain the same fraction of the total variance. This behavior suggests that the influence of SASM on $\delta^{18}O$ may be modulated by ENSO. It is well known that ENSO significantly

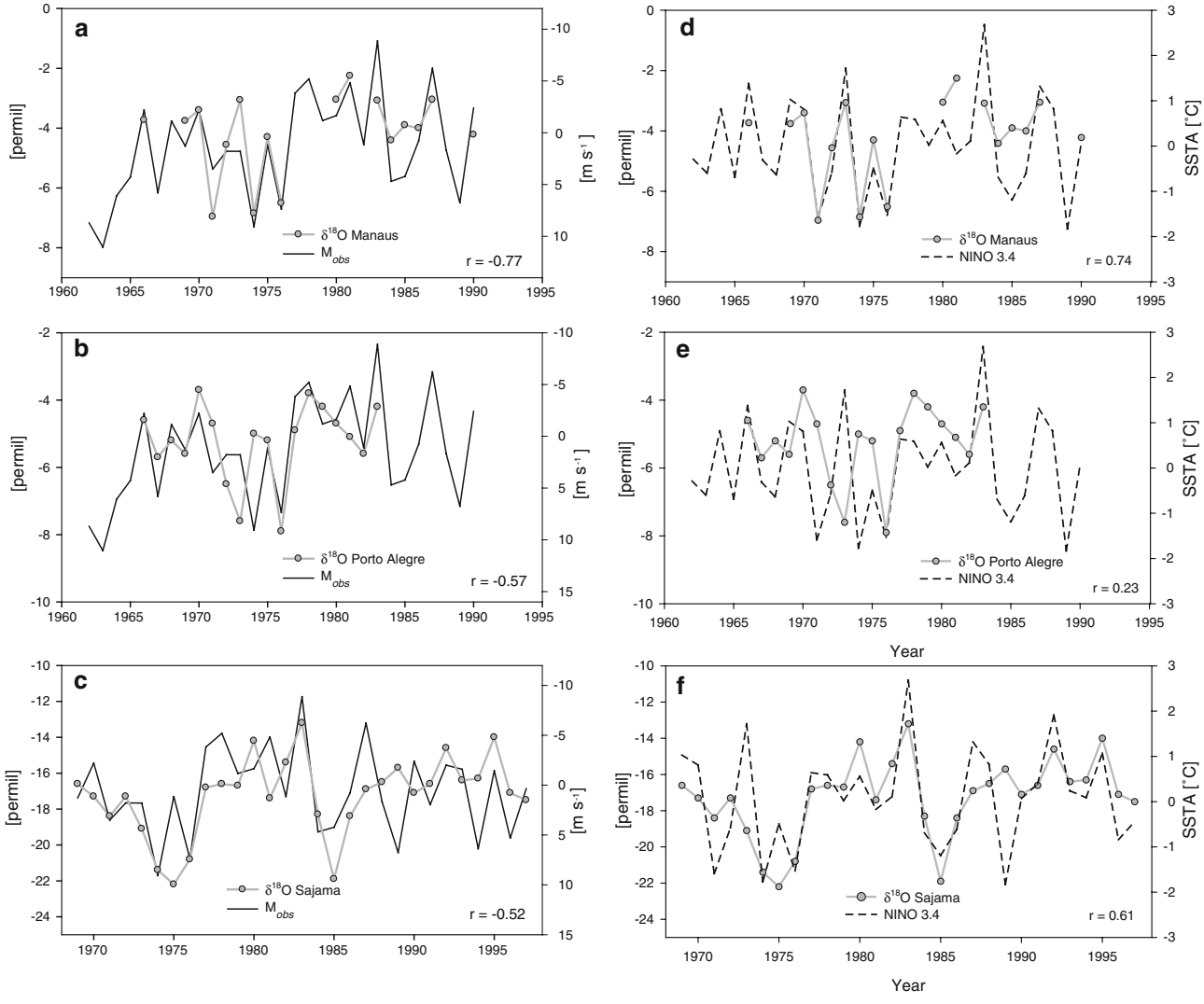

Fig. 7 Comparison between timeseries of M_{obs} and DJF IAEA $\delta^{18}O$ at **a** Manaus (3.12°S, 60.02°W), **b** Porto Alegre (30.08°S, 51.18°W) and **c** Sajama ice cap (18.10°S, 68.88°W). Note that scale for M_{obs} (*right side y*-axis) is reversed. **d**–**f** as in (**a**–**c**) but for comparison with Niño 3.4 index

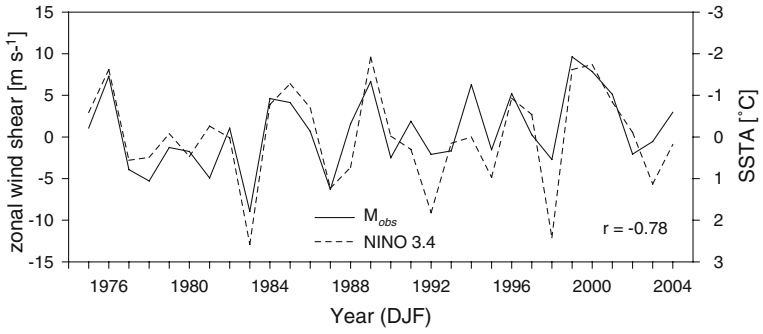

Fig. 8 Comparison between M_{obs} and the Niño-3.4 index. Note that scale for Niño-3.4 index (*right-side y*-axis) is reversed

affects climate and atmospheric circulation over tropical South America during austral summer (e.g. Aceituno 1988, 1989; Vuille 1999; Garreaud and Aceituno 2001; Liebmann and Marengo 2001; Pezzi and Cavalcanti 2001; Zhou and Lau 2001; Coelho et al. 2002; Paegle and Mo 2002; Rao et al. 2002; Ronchail et al. 2002; Lau and Zhou 2003). Indeed SASM and ENSO are highly correlated on interannual timescales (Fig. 8). All this evidence indicates that the apparent relationship between SASM and the stable isotopic composition of summer precipitation may be significantly influenced by tropical Pacific SSTA.

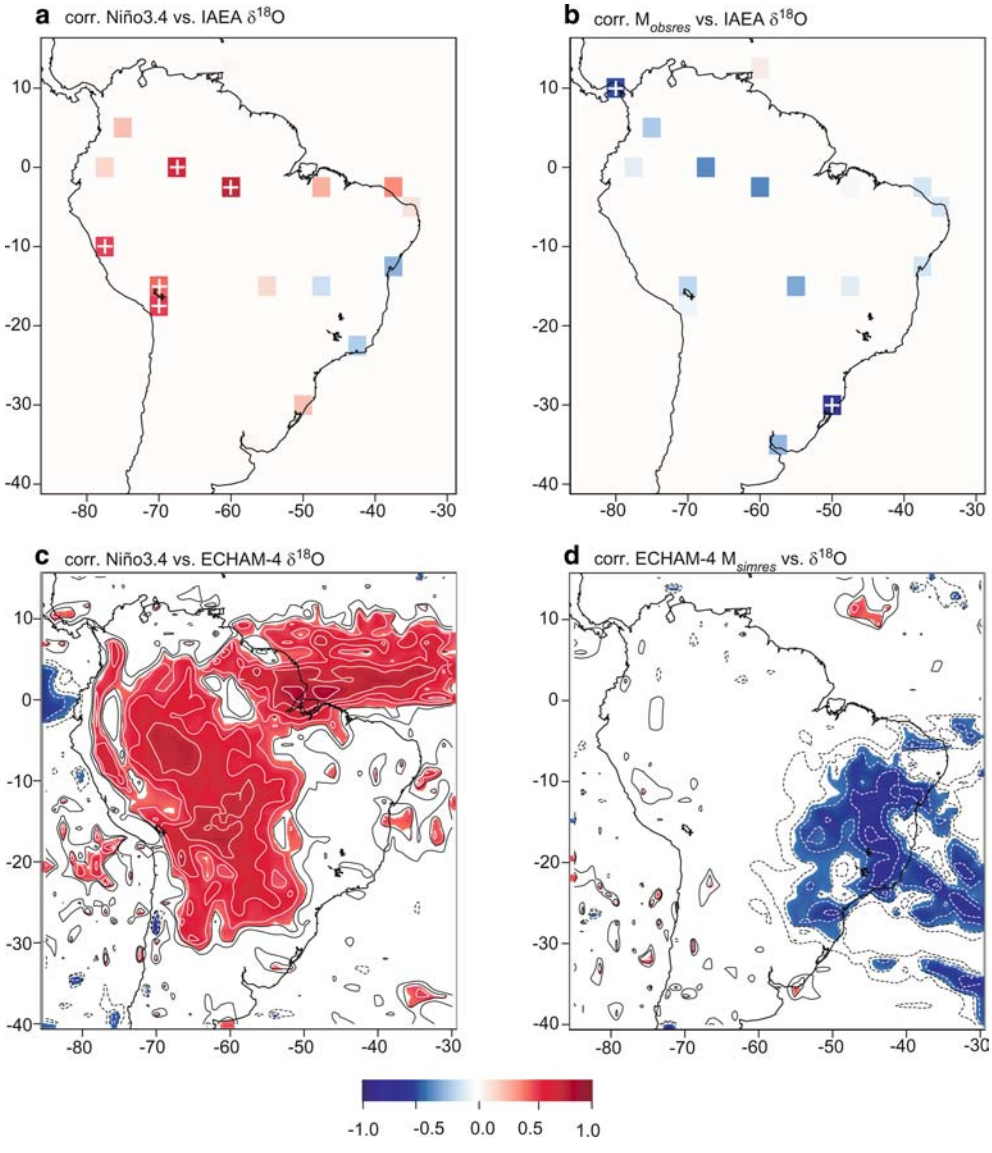

Fig. 9 **a** Correlation of Niño 3.4 with DJF IAEA $\delta^{18}O$ and ice core $\delta^{18}O$ from Huascarán, Quelccaya and Sajama (varying record lengths), **b** as in **a** but for correlation with M_{obsres}, **c** correlation of Niño 3.4 with ECHAM-4 T106 $\delta^{18}O$ (1979–1998), **d** correlation of M_{simres} with ECHAM-4 T106 $\delta^{18}O$ (1979–1998). Significant correlations ($p = 0.05$) in (**a**–**b**) are indicated with *white cross*. Contour interval in (**c**–**d**) is 0.1; contours between 0.2 and −0.2 are omitted; *negative contours* are *dashed*, and significant negative (*positive*) correlations ($p = 0.05$) are *shaded in blue* (*red*)

To further analyze this question we next decompose the SASM-signal into two components: The fraction of variance which is explained by ENSO and the residual component. This residual record of the SASM is obtained by regressing the ENSO index Niño 3.4 against M_{obs} and then retaining the residuals of the linear square fit. This method assumes a linear relationship between ENSO and the SASM, and is therefore a rather crude description of an interaction, which in reality is much more complex. Nonetheless it provides for a first-order approximation of the ENSO-SASM relationship, which can reveal where the SASM-stable isotope relationship is influenced by ENSO. In Fig. 9 we repeat the previous exercise from Fig. 6, but this time correlate the stable isotope data with ENSO (Niño 3.4) and the residual monsoon index, M_{obsres} and M_{simres}, respectively. The correlation of $\delta^{18}O$ from the IAEA-GNIP network and from Andean ice cores with the Niño 3.4 index (Fig. 9a) yields almost the exactly opposite result as compared to the correlation with the SASM (Fig. 6a). Positive correlations prevail, except along the east coast of Brazil between 10°S and 20°S, and the relationship exceeds the 95% significance level over the Amazon basin and the central Andes. In fact Porto Alegre is the only station that is significantly correlated with the SASM but not with ENSO. The correlation of $\delta^{18}O$ with the residual monsoon index, M_{obsres} (Fig. 9b), is consistent with the previously established relationship between $\delta^{18}O$ and the SASM. Correlations are negative throughout the continent, indicating a more depleted stable isotopic composition during summers with more intense monsoons. The significance of this relationship, however, is lowered almost everywhere, once the ENSO-related fraction of the SASM variance is removed. Over the Amazon basin and the central Andes the correlations are no longer significant, suggesting that the interannual variability seen in the tropical Andean ice cores is indeed linked to ENSO, as suggested by Bradley et al. (2003), Hoffmann et al. (2003) and Vuille et al. (2003b). Only Porto Alegre and Howard Air Force Base (8.92°N, 79.60°W) in Panama feature a significant correlation with non-ENSO-related monsoon variability.

The ECHAM-4 model shows results that are very consistent with this observational evidence. ENSO significantly influences the simulated $\delta^{18}O$ variability over the tropical North Atlantic, most of the Amazon basin and the entire tropical and subtropical Andes, with $\delta^{18}O$ being significantly more enriched during El Niño summers and more depleted during La Niña events (Fig. 9c). These are the same regions which also show a significant reduction in precipitation during El Niño events in both model and observations (not shown). There is a clear spatial separation in the model with ENSO-variability being more important to explain $\delta^{18}O$ variations over the northern and western part of the continent, while the residual monsoon influence is stronger over the southeastern part of the continent (Fig. 9d). Hence the significant relationship between non ENSO-related monsoon variability and $\delta^{18}O$ variations in Porto Alegre is confirmed by the model. The significant negative correlations extending into the tropical South Atlantic in our model (Fig. 9d) are also corroborated by observations, which reveal a significant negative correlation between M_{obsres} and $\delta^{18}O$ just outside the domain of our

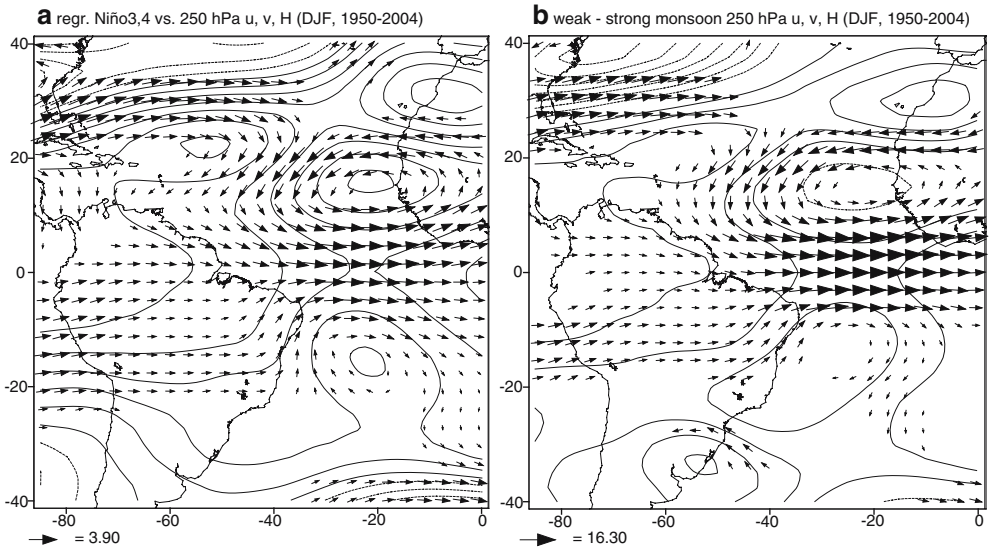

Fig. 10 **a** DJF Niño 3.4 index regressed against 250 hPa wind and geopotential height. Contour interval is 3 gpm per SD; negative contours are *dashed*. Scale for wind vectors is shown in *lower left* (in m s^{-1} per SD). Vectors are only shown if either zonal or meridional component is significantly correlated with Niño 3.4 index at $p = 0.05$. **b** the DJF 250 hPa composite difference of wind and geopotential height during five weakest (1976/1977, 1977/1978, 1980/1981, 1982/1983, 1986/1987) minus five strongest (1961/1962, 1962/1963, 1973/1974, 1998/1999, 1999/1900) monsoon years between 1950 and 2004 as defined by M_{obs}. Contour interval is 10 gpm; negative contours are dashed. Scale for wind vectors (in m s^{-1}) is shown in *lower left*. Vectors are only shown if difference between weak and strong monsoon years is significant at $p = 0.05$ based on two-tailed Student's *t* test

study in the tropical Atlantic on Ascension Island (7.92°S, 14.42°W, not shown). In conclusion these results suggest that a significant fraction of the interannual SASM variability is influenced by tropical Pacific SSTA.

The monsoon index as defined here, is only affected by changes of the atmospheric circulation over the tropical North Atlantic region. To illustrate the remote ENSO impact on tropical Atlantic climate variability, we regress the Niño 3.4 index against DJF upper-tropospheric circulation. Figure 10a shows the wind and geopotential height anomaly associated with a unit anomaly in the Niño 3.4 timeseries. These results are compared with composites of the same variables (Fig. 10b) based on the difference between the five weakest and the five strongest (weak–strong) monsoon summers in the M_{obs} timeseries. These composites thus essentially reflect the conditions characteristic of weak monsoon summers. The equatorial upper- level westerly winds over the Atlantic are significantly enhanced during the ENSO warm phase as is the typical strengthening of the subtropical jet during El Niño events (Fig. 10a). A pair of subtropical cyclones straddling the equator reflects the dynamic response to suppressed convection over the Amazon and the Atlantic ITCZ. This pattern is part of the strong perturbation of the Walker circulation which occurs over the region during El Niño events. The comparison of the Niño 3.4 regression field (Fig. 10a) with the weak monsoon composite (Fig. 10b) leaves little doubt about the significant impact of the remote ENSO forcing. This ENSO impact upon the atmospheric circulation over the tropical Atlantic is part of an "atmospheric bridge" (Klein et al. 1999; Saravanan and Chang 2000; Giannini et al. 2001), linked to anomalous equatorial east–west overturning in response to the warming of the eastern equatorial Pacific (Zhou and Lau 2003).

In summary Fig. 10 provides clear evidence of a strong ENSO influence on the upper air atmospheric circulation over tropical South America and the tropical Atlantic. The most significant influence is located in the region of strongest vertical shear, used to define the SASM in Sect. 3. It therefore comes as no surprise that much of the variance in the SASM record is related to ENSO.

6 Discussion and conclusions

The SASM is an important feature of South American climate and has been recorded in a number of stable isotopic records across the continent. There is however no unified view as to how these records should be interpreted. Here we show how interannual variations in the intensity of the SASM and ENSO influence $\delta^{18}O$ in precipitation based on both observational data and AGCM simulations. There is a significant negative relationship between $\delta^{18}O$ and SASM strength over the Amazon basin, SE South America and the central Andes. While this is entirely consistent with the well-known "amount effect," our results indicate that the degree of rainout upstream may be equally important to explain interannual variations in $\delta^{18}O$.

Our results further suggest that a significant fraction of the interannual SASM variability is remotely forced by tropical Pacific SSTA. ENSO induces significant atmospheric circulation anomalies over the tropical Atlantic and South America, which affects both SASM precipitation and $\delta^{18}O$ variability. Therefore many regions of South America show only a weak relationship between SASM and $\delta^{18}O$, once the SASM signal is decomposed into its ENSO-, and non-ENSO-related variance. The ENSO impact is particularly important over the northern and western part of tropical South America. Impacts of the SASM on the $\delta^{18}O$ record, which are not intertwined with ENSO effects, can mainly be found on the northern border of the South American continent (e.g. Panama), in the region around Porto Alegre, and the tropical South Atlantic. Our findings are consistent with the results of Hoffmann et al. (2003), who emphasized the coherence between century-long records of $\delta^{18}O$ in tropical Andean ice cores and the stable isotopic composition of mid-tropospheric water vapor upstream, and with the results by Vuille et al. (2003b) and Bradley et al. (2003), who argued for a strong impact of ENSO on the $\delta^{18}O$ variability in these ice cores.

There are of course many different ways in which one can define monsoon variability. It is important to keep in mind that results may vary somewhat, depending on what definition is used. The ENSO impact on the atmospheric circulation over the tropical Atlantic—South American domain, for example, is much stronger in the upper than in the lower troposphere. Hence a monsoon definition based solely on the low level circulation, as proposed in previous studies, may yield different results, with a weaker ENSO influence on the SASM.

In addition our simulation focuses on interannual variability only and is limited to a rather short time period during which El Niño events were unusually strong and frequent. Clearly longer observational records and simulations are needed to confirm our results, and to see whether the relationship between ENSO and the SASM undergoes longer term (decadal-scale) variations, which we cannot capture with our short simulation. The fact that our monsoon-index does not accurately capture convective activity over tropical South America during La Niña events is an additional limitation of our study. This may be related to nonlinear interactions between ENSO and the SASM, for which a linear regression method is not an adequate analytical tool. Composite analyses, which consider the influence of El Niño and La Niña events on SASM separately, may be able to address this problem, but they will require longer observational stable isotope records than are currently available. New, more sophisticated simulations, which include an SST—forcing in either the tropical Atlantic or Pacific

basin only (Kelley and Hoffmann 2004) may also help to solve this problem.

An additional consideration is in order with regard to the timing of the SASM. Here we only considered monsoon variability during the mature phase (DJF) of the SASM. However, monsoon variability can also impact precipitation amounts and stable isotopes through changes in the duration or the seasonality (Cruz et al. 2005b). Marengo et al. (2001) have documented how the onset and demise of the rainy season shows considerable interannual variations over tropical South America. On longer time scales this issue is particularly relevant for tropical ice cores, which today show such a strong seasonal bias toward the wet season (Hardy et al. 2003). It is conceivable that the stable isotopic composition could change considerably due to a shift in monsoon seasonality or length of the monsoon season.

Finally, from a paleo-perspective, it is important to emphasize the considerable spatial variability associated with the SASM. While an intensification of the summer monsoon may be recorded as increased wetness in one region, it may lead to increased aridity in another location. Similarly the stable isotopes may not record changes in SASM intensity or location in a similar fashion throughout tropical South America.

Acknowledgements This paper benefited from many long discussions with Francisco Cruz Jr. NCEP-NCAR reanalysis, CMAP precipitation and NOAA interpolated OLR data were all provided by the NOAA CIRES Climate Diagnostics Center. ECHAM simulations were performed with support of the German Climate Computing Center (DKRZ) in Hamburg, Germany. Three anonymous reviewers provided valuable comments, which helped to improve an earlier version of this manuscript. This study was funded by the National Science Foundation (ATM-0317693).

References

Abbott MA, Wolfe BB, Aravena R, Wolfe A, Seltzer G (2000) Holocene hydrological reconstructions from stable isotopes and paleolimnology, Cordillera Real Bolivia. Q Sci Rev 19:1801–1820

Aceituno P (1988) On the functioning of the Southern Oscillation in the South American sector. Part I: surface climate. Mon Wea Rev 116:505–524

Aceituno P (1989) On the functioning of the Southern Oscillation in the South American Sector. Part II: upper-air circulation. J Clim 2:341–355

Baker PA, Seltzer GO, Fritz SC, Dunbar R, Grove MJ, Tapia PM, Cross SL, Rowe HD, Broda JP (2001) The history of South American tropical precipitation for the past 25,000 years. Science 291:640–643

Betancourt JL, Latorre C, Rech JA, Quade J, Rylander KA (2000) A 22,000-yr record of monsoonal precipitation from northern Chile's Atacama desert. Science 289:1542–1546

Bradley RS, Vuille M, Hardy DR, Thompson LG (2003) Low latitude ice cores record Pacific sea surface temperatures. Geophys Res Lett 30(4):1174. DOI 10.1029/2002GL016546

Chou C, Neelin JD (2001) Mechanisms limiting the southward extent of the South American summer monsoon. Geophys Res Lett 28:2433–2436

Coelho CAS, Uvo CB, Ambrizzi T (2002) Exploring the impacts of the tropical Pacific SST on the precipitation patterns over South America during ENSO periods. Theor Appl Climatol 71:185–197

Costa MH, Foley JA (1998) A comparison of precipitation datasets for the Amazon basin. Geophys Res Lett 25: 155–158

Cruz Jr FW, Burns SJ, Karmann I, Sharp WD, Vuille M, Cardoso AO, Silva Dias PL, Ferrari JA, Viana Jr O (2005a) Insolation-driven changes in atmospheric circulation over the past 116,000 years in subtropical Brazil. Nature 434:63–66

Cruz Jr FW, Karmann I, Viana Jr O, Burns SJ, Ferrari JA, Vuille M, Moreira MZ, Sial AN (2005b) Stable isotope study of cave percolation waters in subtropical Brazil: implications for paleoclimate inferences from speleothems. Chem Geology (in press)

Dansgaard W (1964) Stable isotopes in precipitation. Tellus 16:436–468

Enfield DB (1996) Relationship of inter-American rainfall to tropical Atlantic and Pacific SST variability. Geophys Res Lett 23:3305–3308

Fritz SC, Baker PA, Lowenstein T, Seltzer GO, Rigsby CA, Dwyer GS, Tapia PM, Arnold KK, Ku TL, Luo S (2004) Hydrologic variation during the last 170000 years in the southern hemisphere tropics of South America. Q Res 61:95–104

Gan MA, Kousky VE, Ropelewski CF (2004) The South American monsoon circulation and its relationship to rainfall over west-central Brazil. J Clim 17:47–66

Garreaud R, Aceituno P (2001) Interannual rainfall variability over the South American Altiplano. J Clim 14:2779–2789

Garreaud RD, Wallace JM (1998) Summertime incursions of midlatitude air into subtropical and tropical South America. Mon Wea Rev 126:2713–2733

Garreaud R, Vuille M, Clement A (2003) The climate of the Altiplano: Observed current conditions and mechanisms of past changes. Palaeogeogr Palaeoclimatol Palaeoecol 194:5–22

Giannini A, Chiang JCH, Cane M, Kushnir Y, Seager R (2001) The ENSO teleconnection to the tropical Atlantic Ocean: contributions of the remote and local SST's to rainfall variability in the tropical Americas. J Clim 14:4530–4544

Gill AE (1980) Some simple solutions for heat-induced tropical circulation. Q J Roy Meteor Soc 106:447–462

Godfrey LV, Jordan TE, Lowenstein TK, Alonso RL (2003) Stable isotope constraints on the transport of water to the Andes between 22°and 26°S during the last glacial cycle. Palaeogeogr Palaeoclimatol Palaeoecol 194:299–317

Grimm AM (2003) The El Niño impact on the summer monsoon in Brazil: Regional processes versus remote influences. J Clim 16:263–280

Grimm AM (2004) How do la Niña events disturb the summer monsoon system in Brazil? Clim Dyn 22:123–138

Hardy DR, Vuille M, Bradley RS (2003) Variability of snow accumulation and isotopic composition on Nevado Sajama, Bolivia. J Geophys Res 108:4693. DOI: 10.1029/2003JD003623

Hastenrath S (2001) In search of zonal circulations in the equatorial Atlantic sector from the NCEP-NCAR reanalysis. Int J Climatol 21:37–47

Hastenrath S, Greischar L (1993) Circulation mechanisms related to northeast Brazil rainfall anomalies. J Geophys Res 98:5093–5102

Hoffmann G (2003) Taking the pulse of the tropical water cycle. Science 301:776–777

Hoffmann G, Werner M, Heimann M (1998) Water isotope module of the ECHAM atmospheric general circulation model: A study on timescales from days to several years. J Geophys Res 103:16871–16896

Hoffmann G, Ramirez E, Taupin JD, Francou B, Ribstein P, Delmas R, Duerr H, Gallaire R, Simoes J, Schotterer U, Stievenard M, Werner M (2003) Coherent isotope history of Andean ice cores over the last century. Geophys Res Lett 30:4. DOI: 10.1029/2002GL014870

IAEA/WMO (2004) Global Network of Isotopes in Precipitation. The GNIP Database. Accessible at: http://isohis.iaea.org

Kalnay E, Kanamitsu M, Kistler R, Collins W, Deaven D, Gandin L, Iredell M, Saha S, White G, Woollen J, Zhu Y, Chelliah M, Ebisuzaki W, Higgins W, Janowiak J, Mo KC, Ropelewski C,

Wang J, Leetmaa A, Reynolds R, Jenne R, Joseph D (1996) The NCEP/NCAR 40-year reanalysis project. Bull Am Meteorol Soc 77:437–471

Kelley M, Hoffmann G (2004) Isolating the tropical Pacific and Atlantic influences upon simulated Amazonian hydrology and water isotopes. Eos Trans AGU 85(47), Fall Meet Suppl (Abstract C51B-1046)

Klein AS, Soden BJ, Lau NC (1999) Remote sea surface temperature variations during ENSO: Evidence for a tropical atmospheric bridge. J Clim 12:917–932

Koster RD, Dirmeyer PA, Guo Z, Bonan G, Chan E, Cox P, Gordon CT, Kanae S, Kowalczyk E, Lawrence D, Liu P, Lu CH, Malyshev S, McAvaney B, Mitchell K, Mocko D, Oki T, Oleson K, Pitman A, Sud YC, Taylor CM, Verseghy D, Vasic R, Xue Y, Yamada T (2004) Regions of strong coupling between soil moisture and precipitation. Science 305:1138–1140

Lau KM, Zhou H (2003) Anomalies of the South American summer monsoon associated with the 1997–99 El Niño-Southern Oscillation. Int J Climatol 23:529–539

Lenters JD, Cook KH (1997) On the origin of the Bolivian High and related circulation features of the South American Climate. J Atmos Sci 54:656–677

Liebmann B, Marengo JA (2001) Interannual variability of the rainy season and rainfall in the Brazilian Amazon basin. J Clim 14:4308–4318

Liebmann B, Smith CA (1996) Description of a complete (interpolated) outgoing longwave radiation dataset. Bull Am Meteorol Soc 77:1275–1277

Liebmann B, Marengo JA, Glick JD, Kousky VE, Wainer IC, Massambani O (1998) A comparison of rainfall, outgoing longwave radiation and divergence over the Amazon basin. J Clim 11:2898–2909

Marengo JA, Hastenrath S (1993) Case studies of extreme climatic events in the Amazon basin. J Clim 6:617–627

Marengo JA, Liebmann B, Kousky VE, Filizola NP, Wainer IC (2001) Onset and end of the rainy season in the Brazilian Amazon basin. J Clim 14:833–852

Mechoso CR, Lyons SW, Spahr JA (1990) The impact of sea surface temperature anomalies on the rainfall over northeast Brazil. J Clim 3:812–826

Oyama MD, Nobre CA (2003) A new climate-vegetation equilibrium state for tropical South America. Geophys Res Lett 30:2199. DOI:10.1029/2003GL018600

Paegle JN, Mo KC (2002) Linkages between summer rainfall variability over South America and sea surface temperature anomalies. J Clim 15:1389–1407

Pezzi LP, Cavalcanti IFA (2001) The relative importance of ENSO and tropical Atlantic sea surface temperature anomalies for seasonal precipitation over South America: a numerical study. Clim Dyn 17:205–212

Ramirez E, Hoffmann G, Taupin JD, Francou B, Ribstein P, Caillon N, Ferron FA, Landais A, Petit JR, Pouyaud B, Schotterer U, Simoes JC, Stievenard M (2003) A new deep ice core from Nevado Illimani (6350 m). Earth Planet Sci Lett 212:337–350

Rao VB, Santo CE, Franchito SH (2002) A diagnosis of rainfall over South America during the 1997/98 El Nino event. Part I: Validation of NCEP-NCAR reanalysis rainfall data. J Clim 15:512–521

Ronchail J, Cochonneau G, Molinier M, Guyot JL, Chaves AGDM, Guimaraes V, De Oliveira E (2002) Interannual rainfall variability in the Amazon basin and sea surface temperatures in the equatorial Pacific and the tropical Atlantic Oceans. Int J Climatol 22:1663–1686

Rowe HD, Dunbar RB (2004) Hydrologic energy balance constraints on the Holocene lake-level history of Lake Titicaca, South America. Clim Dyn 23:439–454

Saravanan R, Chang P (2000) Interaction between tropical Atlantic variability and El Niño-Southern Oscillation. J Clim 13:2177–2194

Seltzer G, Rodbell D, Burns S (2000) Isotopic evidence for late quaternary climatic change in tropical South America. Geology 28:35–38

Seluchi ME, Marengo JA (2000) Tropical-midlatitude exchange of air masses during summer and winter in South America: Climatic aspects and examples of intense events. Int J Climatol 20:1167–1190

Silva Dias PL, Schubert WH, Demaria M (1983) Large-scale response of the tropical atmosphere to transient convection. J Atmos Sci 40:2689–2707

Thompson LG, Mosley-Thompson E, Bolzan JF, Koci BR (1985) A 1500 year record of tropical precipitation in ice cores from the Quelccaya ice cap, Peru. Science 229:971–973

Thompson LG, Mosley-Thompson E, Davis ME, Lin PN, Henderson KA, Cole-Dai J, Bolzan JF, Liu KB (1995) Late glacial stage and Holocene tropical ice core records from Huascaran, Peru. Science 269:46–50

Thompson LG, Davis ME, Mosley-Thompson E, Sowers TA, Henderson KA, Zagorodnov VS, Lin PN, Mikhalenko VN, Campen RK, Bolzan JF, Cole-Dai J, Francou B (1998) A 25,000-Year tropical climate history from Bolivian Ice cores. Science 282:1858–1864

Trenberth K (1997) The definition of El Niño. Bull Am Meteorol Soc 78:2771–2777

Uvo BC, Repelli CA, Zebiak SE, Kushnir Y (1998) The relationships between tropical Pacific and Atlantic SST and Northeast Brazil monthly precipitation. J Clim 11:551–562

Vuille M (1999) Atmospheric circulation over the Bolivian Altiplano during dry and wet periods and extreme phases of the Southern Oscillation. Int J Climatol 19:1579–1600

Vuille M, Bradley RS, Keimig F (2000a) Climatic variability in the Andes of Ecuador and its relation to tropical Pacific and Atlantic sea surface temperature anomalies. J Clim 13:2520–2535

Vuille M, Bradley RS, Keimig F (2000b) Interannual climate variability in the central Andes and its relation to tropical Pacific and Atlantic forcing. J Geophys Res 105:12447–12460

Vuille M, Bradley RS, Werner M, Healy R, Keimig F (2003a) Modeling $\delta^{18}O$ in precipitation over the tropical Americas: 1. Interannual variability and climatic controls. J Geophys Res 108:4174. DOI:10.1029/2001JD002038

Vuille M, Bradley RS, Healy R, Werner M, Hardy DR, Thompson LG, Keimig F (2003b) Modeling $\delta^{18}O$ in precipitation over the tropical Americas: 2. Simulation of the stable isotope signal in Andean ice cores. J Geophys Res 108(D6):4175. doi:10.1029/2001JD002039

Wagnon P, Sicart JE, Berthier E, Chazarin JP (2003) Wintertime high-altitude surface energy balance of a Bolivian glacier, Illimani, 6340 m above sea level. J Geophys Res 108:6. DOI: 10.1029/2002JD002088

Wang B, Fan Z (1999) Choice of South Asian summer monsoon indices. Bull Am Meteorol Soc 80:629–638

Webster PJ, Yang S (1992) Monsoon and ENSO: selective interactive systems. Q J Royal Meteorol Soc 118:877–926

Xie P, Arkin PA (1997) Global precipitation: a 17-year monthly analysis based on gauge observations, satellite estimates, and numerical model outputs. Bull Am Meteorol Soc 78:2539–2558

Zhou J, Lau KM (1998) Does a monsoon climate exist over South America? J Climate 11:1020–1040

Zhou J, Lau KM (2001) Principal modes of interannual and decadal variability of summer rainfall over South America. Int J Climatol 21:1623–1644